Large zenith-angle observations with the CAT Cherenkov imaging telescope

G. Mohanty[1] **for the CAT Collaboration**

LPNHE, Ecole Polytechnique and IN2P3/CNRS, Palaiseau, France

Abstract

We present here results from large zenith-angle observations with the CAT atmospheric Cherenkov imaging telescope, based on data taken on the Crab Nebula and on the blazar Mk501 from 1996 onwards. From Monte Carlo simulations, the threshold energy of the telescope is expected to vary from about 250 GeV at zenith to about 2 TeV at a zenith angle of $60°$. The lower source-fluxes due to the increased threshold energy are partly compensated for by an increase in the effective collection area at large zenith angles, thus allowing a significant extension of the dynamic range of the CAT telescope, with a tolerable loss in sensitivity. We discuss the implications for source detection and energy spectrum measurements.

1   Introduction:

The CAT atmospheric Cherenkov imaging telescope (Barrau et al., 1998) has been operating from 1996 onwards at the site of a former solar plant, Thémis, in the French Pyrénées. It achieves a low energy threshold of about 250 GeV at the zenith, in spite of a relatively small mirror area of 17.7 m^2, by discriminating against the night-sky background with the rapid timing made possible by the near-isochronous mirror, fast photomultipliers, and high-speed trigger and readout electronics. It also uses a high-definition camera, with a central region of 546 pixels of $0.12°$ each, that allows the use of a powerful χ^2 image-analysis technique (LeBohec et al., 1998) which very effectively rejects background shower images while also offering excellent source location and energy resolution for gamma-ray images. The CAT telescope has detected gamma-ray emission from the Crab Nebula (Iacoucci et al., 1998) and from the extra-galactic BL Lac objects, Mk501 (Djannati-Ataï et al., 1999. Also, see OG.2.1.08, these proceedings) and Mk421 (described in OG.2.1.09, these proceedings). This paper discusses the use of the telescope for large zenith-angle (here, $> 35°$, unless otherwise indicated) observations on the Crab Nebula and on Mk501.

Large zenith-angle (LZA) observations of the Cherenkov light from air-showers were originally proposed by Sommers & Elbert (1987) as a means of increasing the effective detection area. The technique has since been successfully applied to a variety of instruments (e.g., Krennrich et al., 1997, Krennrich et al., 1999, Tanimori et al., 1998) Due to the greatly increased sensitivity at higher threshold energies, this technique enables the study of the high-energy end of source spectra which is interesting for various purposes, such as the modelling of the gamma-ray emission mechanism at the source, measurement of the infra-red intergalactic photon density, etc.

2   The large zenith-angle technique

For large zenith-angle observations, the particle cascade in the air-shower develops relatively farther away from the telescope, and furthermore, the Cherenkov light from an air-shower is seen through a larger atmospheric depth. This implies a higher detection energy threshold for a trigger based on the photon density at ground level, which leads to a decrease in the observed flux from observed TeV gamma-ray sources that exhibit spectra falling sharply with energy. The lower source fluxes are compensated for by the increase in the effective detector area resulting both from the effect of geometrical projection onto the ground and from the shower being more highly developed at the observatory level. Also, as the maximum of shower development is further away from the telescope, the images at a given energy are smaller and fainter, with a lower signal-to-noise ratio. This change in the image parameter distributions need to be taken into account in the gamma-ray selection cuts. The calibration of the detector at large zenith angles is also more complicated as the data are more sensitive to fluctuating weather conditions.

3 Simulations and data analysis

Data were taken on the three sources above in the usual ON/OFF mode, where the source is tracked for about 28 min., then the telescope is slewed back and is used to observe a control region covering the same range of right-ascension and declination. In general, more data are taken ON-source than OFF-source. The data quality is constantly monitored for changing weather conditions and electronic problems, and the conversion efficiency from Cherenkov photons at ground level to photoelectrons is regularly measured. This enables us to select data taken under stable observing conditions, with, typically, 75% of the data runs being deemed suitable for analysis. Here, the data are analysed by two independent methods to guard against systematic effects at large zenith angles. The first is the usual sophisticated χ^2 analysis, which automatically takes the effect of the zenith angle into account, with the cuts being: $P(\chi^2) > 0.35$, $\alpha < 6°$, along with a cut on the total charge, $Q_{tot} > 30$ pe, that rejects low-light images. The second method is extended supercuts (Mohanty et al., 1998), which uses the usual Hillas parameters but allows them to scale with Q_{tot}. For the second method, simulated gamma-rays and background from data are used to optimize the passbands for the various parameters at several discrete zenith angles and these are then interpolated to all zenith angles. All available data on the two sources up to the end of April 1999 has been considered.

Gamma-ray showers have been simulated with the KASCADE shower simulation program (Kertzman & Sembroski, 1994), modified locally by G. Vacanti and E. Pare. The response of the CAT detector is simulated by other programs that include a comprehensive modelling of the telescope optics and electronics. All simulations have been validated on the strong gamma-ray signal observed from Mk501 in April 1997, when it was at an extremely high-flux level.

Simulated showers were generated with primary energies from 0.05 TeV to 10 TeV, drawn from a power-law distribution with a -2.25 differential index, and scattered uniformly over a circle of 250 m radius. Fig. 1 compares the distributions of Q_{tot} and the Hillas parameter, $width$, from the simulations, at $0°$ and $55°$, to those from the excess in data taken on Mk501 in a high state, centred on the corresponding zenith angles. Both simulations and data have been selected only by $\alpha < 6°$, and all distributions have been renormalized to have the same (arbitrary) total number of events. The agreement is seen to be good at both zenith angles, though the statistics at $55°$ are limited. The distributions also illustrate the expected effect of fainter and smaller images at larger zenith angles.
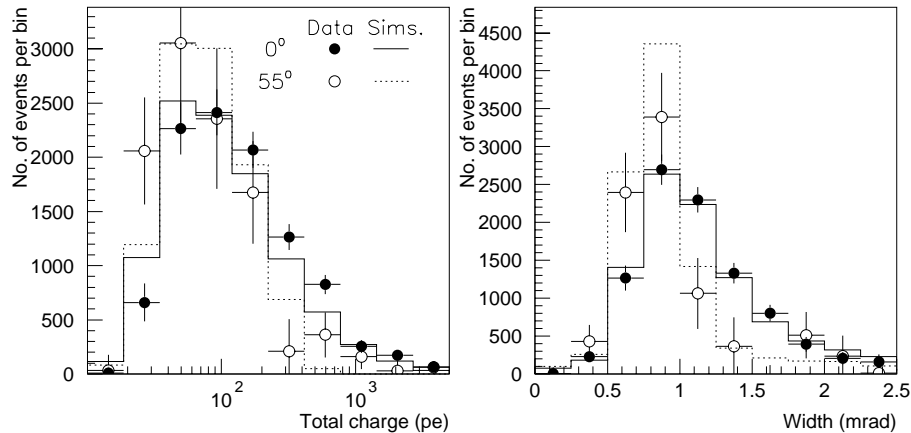
Figure 1: Comparison of parameter distributions from simulations and data at two different zenith angles.

Fig. 2(a) shows the dramatic change in the effective detector area, before the application of gamma-ray cuts, calculated from simulations at several different zenith angles. The detector threshold energy is conventionally defined as the peak of the expected telescope event rates for a source with a power-law spectrum of differential index -2.7, being only weakly dependent on the assumed index. The threshold energies thus defined, are, 0.24 TeV at $0°$, 0.35 TeV at $30°$, 0.70 TeV at $45°$, and 2.2 TeV at $60°$. Fig. 2(b) has two panels comparing

the gamma-ray rate, and the significance for a Crab-like source observed at different zenith angles. The lines indicate the expected values calculated from the known background rate as a function of zenith angle, and from gamma-ray simulations for a Crab-like source. The points are experimental values for the excesses on the Crab obtained at various zenith angles. (As the Crab culminates at about $20°$ at Thémis, the points are limited to zenith angles above that.) The rates and significances are seen to be in good agreement for both methods, except at very large zenith angles. Also, it should be noted that the increase in detector area compensates to a large extent for the increase in the energy threshold, the decrease in the gamma-ray rate with zenith angle being much slower than would be otherwise expected.
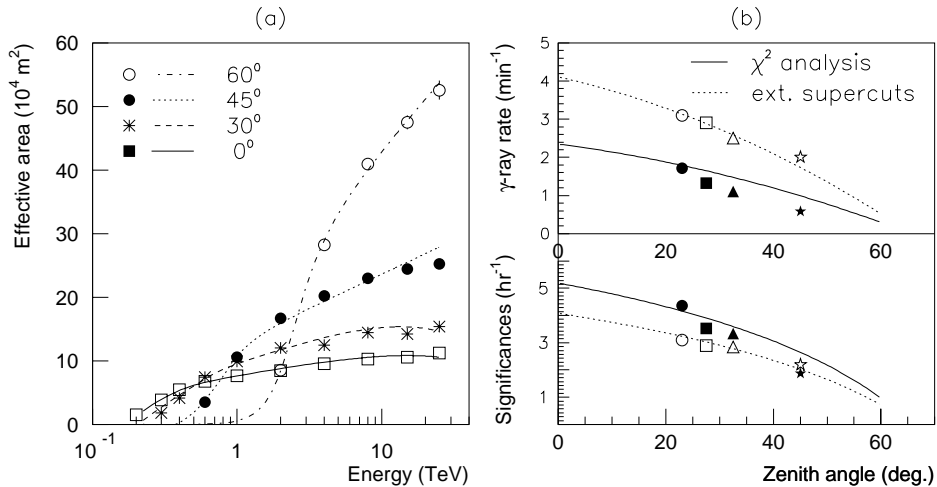
Figure 2: (a) Effective detector area at various zenith angles. (b) γ-ray rates (upper panel) and significances (lower panel) from a Crab-like source. The lines indicate calculated values while data from the Crab Nebula at various zenith angles are shown as points ($< 25°$: circles, $25°$–$30°$: squares, $30°$–$40°$: triangles, and $> 40°$: stars). The solid points are from the χ^2 analysis, and the open ones from extended supercuts.

4   Results

The simulations and data were shown to be in good agreement in the previous section. Fig. 3 presents the excess on the Crab Nebula, at small ($< 25°$) and large ($> 35°$) zenith angles, in the pointing angle, α, after selection on P $\left(\chi^2\right)$ and Q_{tot}. The OFF data has been renormalized by the ratio between the OFF-source and ON-source observation time. The excess at large zenith angles is clearly evident. By further restricting the data to zenith angles above $40°$, one can examine the high-energy end of the flux from the Crab Nebula. From just 9 hours of data above $40°$, we observe a 2σ excess above a reconstructed energy of 10 TeV (this corresponds to a real energy of 7 TeV at the 95% confidence level, assuming a power-law spectrum with a differential spectrum of -2.5). By comparison, one would need about ten times as much observation time below $25°$ to arrive at the same significance at 10 TeV. Observations at large zenith angles also allow the cross-calibration of spectra derived in different zenith angle bins.

Similarly, Fig. 4(a) shows the LZA excess in α for Mk501. The data on Mk501 is dominated by a period of high activity in 1997 which is seen also at very large zenith angles. This enables us to go down to below $40°$ for the flare period as shown in Fig. 4(b). Here also, the excess at large zenith angles is easily visible. The spectrum of MK501 deviates considerably from a power-law spectrum (see, e.g., Krennrich et al. 1999, Djannati-Ataï et al., 1999). This curvature is seen also in the LZA observations, and is presently under investigation.

5   Conclusions

We have demonstrated the ability of the CAT telescope to observe down to large zenith angles, with the excess in the data agreeing fairly well with the simulations. We are in the process of estimating energy spectra

with the LZA technique.

References

Barrau, A., et al. 1998, Nucl. Instrum. Methods Phys. Res., Sect. A, 416, 278

Iacoucci, L., et al., 1998, in Proc. 16th European Cosmic Ray Conference, 363

Kertzman, M., and Sembroski, G., 1994, Nucl. Instrum. Methods Phys. Res., Sect. A, 343, 629

Krennrich, F., et al., 1997, ApJ, 482, 758

Krennrich, F., et al., 1999, ApJ, 511, 149

Lebohec, S., et al., 1998, Nucl. Instrum. Methods Phys. Res., Sect. A, 416, 425

Mohanty, G., et al., 1998, Astrop. Phys., 9, 15

Sommers. P., and Elbert, J. W., 1987, J. Phys. G: Nucl. Phys., 13, 553

Tanimori, T., et al., 1998, 492, L33
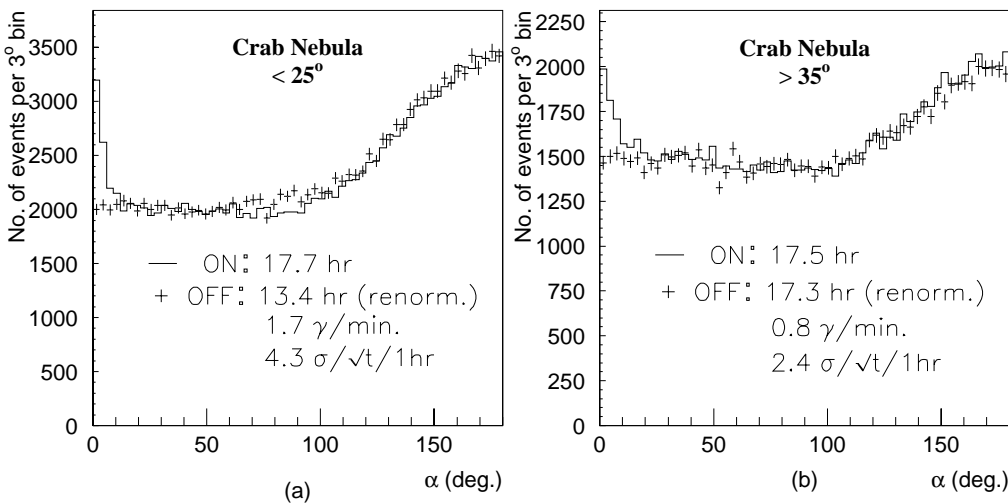
Figure 3: Excess from the Crab Nebula at (a) small, and (b) large zenith angles.
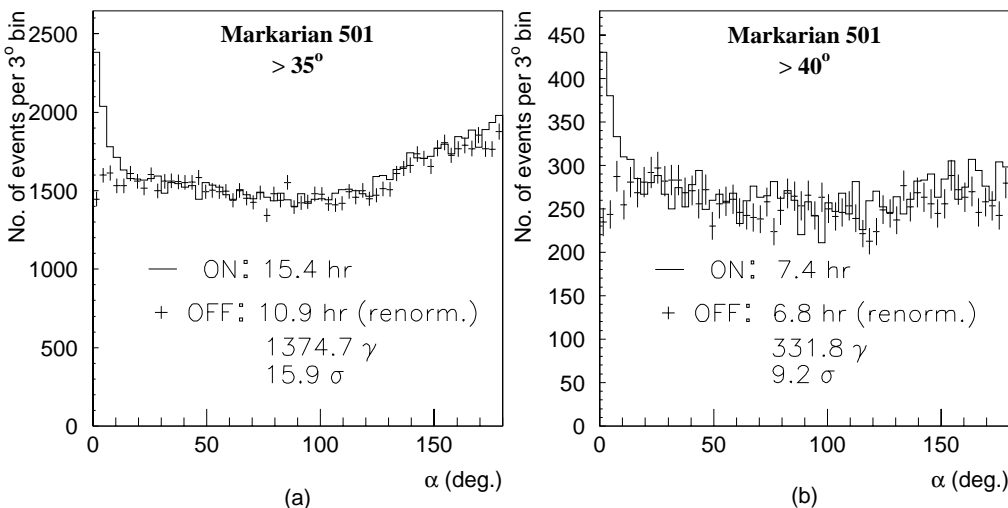
Figure 4: The large zenith-angle excess from Mk421: (a) above $35°$, and, (b) above $40°$.